Modulation of single hyperpolarization-activated channels (i_f) by cAMP in the rabbit sino-atrial node

Dario DiFrancesco* and Matteo Mangoni

Università di Milano, Dipartimento di Fisiologia e Biochimica Generali, Elettrofisiologia, via Celoria 26, 20133 Milano, Italy

1. The hyperpolarization-activated 'pacemaker' current (i_f) was recorded in inside-out patches excised from rabbit sino-atrial (SA) node cell membranes.

2. Single-channel activity could be resolved in patches containing only a few channels; the voltage dependence of single-channel size and single-channel conductance (0·97 pS) were similar to those measured previously in cell-attached conditions.

3. Perfusion of the intracellular side of the patch membrane with 10 μM cAMP facilitated the opening of single i_f channels on hyperpolarization. The cAMP-induced i_f current activation occurred without modification of the single-channel conductance.

4. Modification by cAMP of the probability of channel opening was investigated with respect to the latency to first opening during hyperpolarization and in patches containing a large number of channels (macro-patches). First-latency histograms showed that cAMP shifts the probability curve of first openings to shorter times, in agreement with a cAMP-induced facilitation of channel opening. In macro-patches, measurement of the voltage dependence of the open probability by a slow voltage ramp protocol showed that cAMP shifts the probability curve to more positive voltages without modifying its shape.

5. In cell-free macro-patches the normalized open probability curve in control solutions was centred around −121·9 mV, a voltage some 30 mV more negative than in cell-attached macro-patches. Negative shifting of the curve after patch excision could only partly be explained by the removal of intracellular cAMP, and progressed with time during the ramp protocol, suggesting the presence of a run-down process independent from cAMP.

The hyperpolarization-activated (i_f) current is involved in the generation of spontaneous activity in cardiac pacemaker sino-atrial (SA) node cells (DiFrancesco, 1991). It is modulated in opposite ways by β-adrenergic and cholinergic input, through stimulation and inhibition, respectively, of adenylate cyclase and production of cAMP, which ultimately controls the degree of i_f activation on hyperpolarization. By controlling the rate of development of the diastolic depolarization and consequently the rate of spontaneous activity, i_f modulation by cAMP is thus the key mechanism by which the autonomous nervous system regulates cardiac rhythm (DiFrancesco, 1993).

β-Adrenergic stimulation activates i_f by shifting its activation range to more positive voltages, thereby increasing the degree of current activation at any given voltage (Noble & Tsien, 1968; Brown, DiFrancesco & Noble, 1979; Noma, Kotake & Irisawa, 1980; DiFrancesco, Ferroni, Mazzanti & Tromba, 1986; DiFrancesco & Tromba, 1988*a*). cAMP is the second messenger of i_f control, and acts as if, in the presence of cAMP, the gating mechanism of the channel sensed a higher membrane polarization than in control conditions. Recently, a study of the cAMP action in inside-out patches of SA node membranes has revealed that i_f activation by cAMP does not involve a phosphorylation process, as it does for all other known voltage-gated, cAMP-activated currents (de Peyer, Cachelin, Levitan & Reuter, 1982; Osterrieder, Brum, Hescheler, Trautwein, Flockerzi & Hoffmann, 1982; Reuter, 1983; Levitan, 1985; Shuster, Camardo, Siegelbaum & Kandel, 1985), but rather a direct binding of the cyclic nucleotide to the channel (DiFrancesco & Tortora, 1991). As single i_f channels have a low conductance (about 1 pS, DiFrancesco, 1986) and are not easily resolved, the above result was achieved using macro-patches containing a large number of channels (Yatani, Okabe, Codina, Birnbaumer & Brown, 1990).

However, elementary i_f channel events can indeed be identified in single-pipette cell-attached experiments, although with a lower resolution than in two-pipette experiments (see for example Fig. 3*f–h* in DiFrancesco, 1986), suggesting the possibility that, under appropriate

*To whom reprint requests should be addressed.

conditions, the i_f modulation by cAMP is investigated at the single-channel level. We therefore decided to explore possible favourable conditions to improve the resolution of single i_f channel recording in the inside-out configuration.

Here we show that in inside-out patches containing only a few i_f channels, elementary events can be resolved under favourable conditions and the direct cAMP-induced activation of single i_f channels can be investigated. We find that cAMP increases the probability of channel opening upon hyperpolarization without modifying their conductance, in agreement with previous evidence on β-adrenergic stimulation of single i_f channels in cell-attached conditions. cAMP acts by shifting the voltage dependence of the channel open probability curve to the positive direction (by an average 13·2 mV with 10 μM cAMP), without significantly modifying its slope. This provides the first direct demonstration of the mechanism of activation of single voltage-gated, cyclic-nucleotide-dependent channels by cAMP.

METHODS

Albino rabbits weighing 0·8–1·0 kg were killed by cervical dislocation and exsanguination under respiratory tribromoethanol anaesthesia (200 mg (10 ml ether)$^{-1}$). The SA node region was isolated and single SA node myocytes prepared and stored according to the protocols reported elsewhere (see for example DiFrancesco & Tromba, 1988*a*). Cells under study were harvested in plastic Petri dishes containing a stainless-steel ring to reduce the bath volume to 1 ml, placed on the stage of an inverted microscope and continuously superfused with a high potassium solution containing (mM): KCl, 130; NaCl, 10; $MgCl_2$, 1; Hepes–KOH, 10; and D-glucose, 5 (pH = 7·4). Under these conditions, spontaneous activity was arrested. All experiments were done at the controlled temperature of 27–28 °C.

Single i_f channel recording in cell-free patches

Inside-out patches were formed as described previously (DiFrancesco & Tortora, 1991) using pipettes with resistances of about 5 MΩ when filled with the following solution (mM): NaCl, 70; KCl, 70; $CaCl_2$, 1·8; $MgCl_2$, 1; $BaCl_2$, 1; $MnCl_2$, 2; and Hepes–NaOH, 5 (pH = 7·4). Patches excised in the inside-out configuration were exposed to solutions delivered through a perfusion pipette that allowed solution changes in less than 1 s. Bath inflow was simultaneously turned off. The control solution perfusing the intracellular side of the membrane patches contained (mM): potassium aspartate, 130; NaCl, 10; $CaCl_2$, 2; EGTA, 5; and Hepes–KOH, 10 (pH = 7·2, pCa = 7). After patch excision, pipettes were lifted up in the bath to minimize depth of

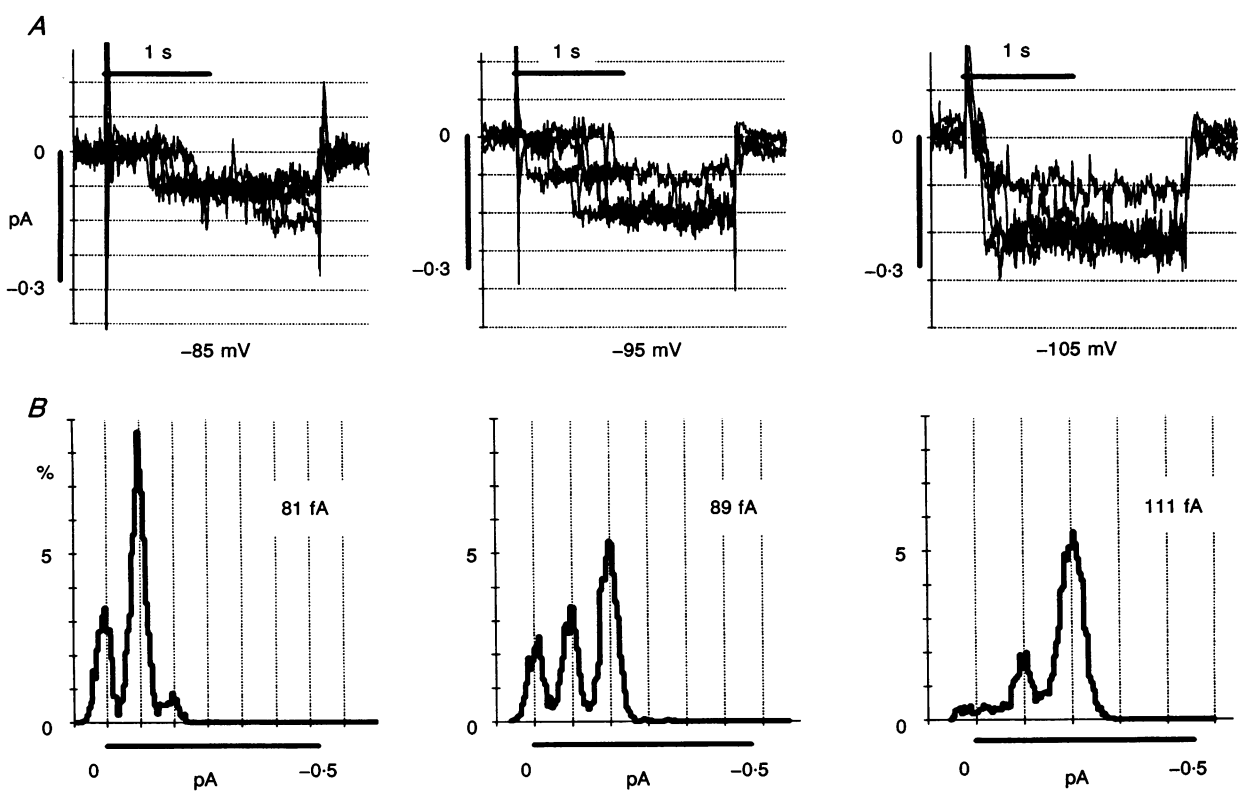

Figure 1. Single i_f channel recording in an inside-out patch from a sino-atrial node cell membrane apparently containing two channels

A, superimposition of current traces recorded during steps from −35 (intracellular side negative) to −85 (left), −95 (middle) and −105 mV (right) after correction for linear capacitative and leak components. Six records are overlapped in each panel. *B*, cumulative histograms (bin = 5 fA) of current distribution (%) in corresponding upper records. Single-channel amplitudes obtained by the histogram peak-fitting procedure explained in the Methods were −81, −89 and −111 fA at −85, −95 and −105 mV, respectively, and were used to draw grids on histogram and current panels.

immersion and voltage clamp steps were delivered to the patch via the bath pellet, while the pipette potential was kept at 0 mV. This substantially reduced the transient due to charging of the pipette capacity, avoided saturation of the current signal, and increased the signal/noise ratio during voltage steps. All traces were corrected for linear capacitative and leakage components. Traces were digitized at 0·75 kHz and filtered through a 4-pole Bessel filter with cut-off frequency of 80–160 Hz. Trans-patch potentials given in this work always conventionally represent intracellular side minus extracellular side potentials. Each average is expressed as mean ± S.E.M. Data presented in this work are based on 27 experiments where 137 patches have been studied.

Measurement of single-channel amplitude

To measure single-channel amplitudes in histogram plots, we used the following procedure: for a given single-channel size (δ), we summed the histogram area of three consecutive bins centred around δ, 2δ, 3δ, ...$N\delta$, N being the maximal number of openings identified by visual inspection of current traces, and maximized the calculated sum as a function of δ (step = 1 fA).

Macro-patches

Macro-patches containing a large number of i_f channels were formed using large-tipped pipettes (resistance of 1–2 MΩ) as previously described (DiFrancesco & Tortora, 1991). Macro-patch i_f steady-state I–V relations were measured by applying hyperpolarizing voltage ramps with a rate of −110 mV min^{-1} from a holding potential of −35 mV, as in Fig. 6, and plotted after leakage correction. Probability curves were then calculated as the ratio between steady-state and fully activated relations. The latter were obtained as linear extrapolations from the peak value at −145 mV to the zero value at a fixed reversal potential of −12·24 mV. This value was selected as the mean reversal potential from $n = 8$ measurements of macro-patch I–V relations (−12·24 ± 0·75 mV); it is very close to the value of −13 mV extrapolated from previously reported cell-attached single-channel measurements (DiFrancesco, 1986). The above method makes the assumption that fully activated I–V relations are linear, and that cAMP does not alter the i_f reversal potential in macro-patches; both conditions are experimentally verified (DiFrancesco & Tortora, 1991). We checked in pilot experiments that prolonging the ramp duration from 60 to 90 s did not alter the position of the probability curve significantly (deviation in $E_{½}$, the mid-activation voltage, was 0·81 ± 0·34 mV, $n = 8$). This indicates that the current recorded with 1 min ramps satisfactorily approximated the steady-state i_f.

The steady-state macro-patch current I is defined as $I = iNp_o$, where i is the single-channel current, N the number of channels in the patch, and p_o the open probability. If p_m is the maximal open probability reached at negative voltages, the curve iNp_m represents the fully activated I–V relation for macro-patch i_f. The ratio between steady-state relation and fully activated curve thus represents the normalized open probability $p_n = p_o/p_m$ (see Fig. 6*C*).

First-latency histograms

For a given set of single-channel recordings from an inside-out patch containing N channels (as determined by visual inspection of single-channel traces under maximizing conditions), the time following onset of the hyperpolarizing step was divided into a grid of 50 ms bins and the cumulative probability histogram curve of first openings constructed by using the following method: let n_i be the number of records where the first opening occurs in the ith bin ($i = 1...q$); then, defining as n_0 the number of traces where no opening occurs (nulls), the cumulative frequency of latency to first opening, W, in the ith bin is calculated as

$$W_i = \left(\sum_{1}^{i} n_j\right) / \left(\sum_{0}^{q} n_j\right). \quad (1)$$

In the case of a large number of channels and of a vanishing bin size, the function $W(t)$ would represent the probability that a first opening is observed by the time t since pulse onset. The routine for automatic detection of channel opening required the measured current to be higher than 70 % of the single-channel amplitude (as determined by amplitude histogram analysis). To exclude further the possibility of fast noise fluctuations being detected as false openings, the detection routine could be adjusted, if necessary, to discard events briefer than a fixed, short time (for example 10 ms).

RESULTS

In Fig. 1, superimpositions of single-channel traces recorded from an inside-out patch are shown during hyperpolarizations to −85, −95 and −105 mV (*A*). Six traces are overlapped in each panel. The patch contained apparently two channels, as judged from the maximal number of openings observed, and elementary events were clearly

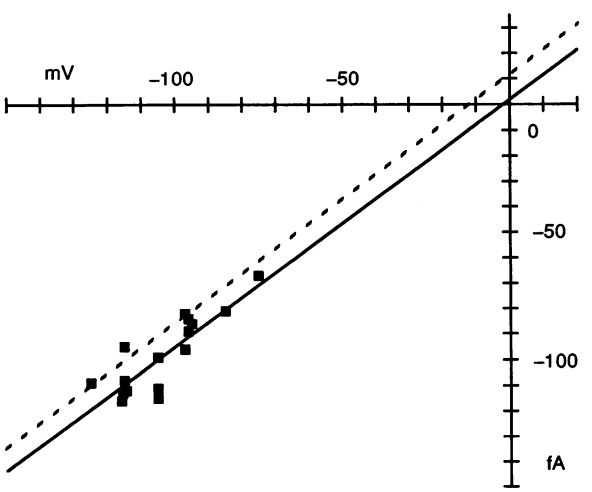

Figure 2. Voltage dependence of single i_f channel amplitudes in inside-out patches
Single-channel amplitudes were measured in $n = 8$ patches by fitting histogram peaks (see Methods). Single-channel conductance and reversal potential calculated from linear regression of data points (continuous line) were 0·97 pS and −1·97 mV, respectively. The I–V relation obtained previously from two-pipette, cell-attached experiments (conductance of 0·98 pS and reversal potential of −13 mV, DiFrancesco, 1986) is also drawn for comparison as a dashed line.

distinguishable. The single-channel amplitudes were measured from the peaks of the histograms of current distribution in Fig. 1*B*, using an algorithm that maximizes the current distribution around peaks, as described in the Methods section. These were −81, −89 and −111 fA at −85, −95 and −105 mV, respectively.

To verify the reliability of our measurements, we compared in Fig. 2 the single-channel amplitudes obtained from inside-out patches (squares) with the results of previous cell-attached measurements with the two-pipette method drawn as a dashed line (DiFrancesco, 1986). The agreement between data from the two protocols appears to

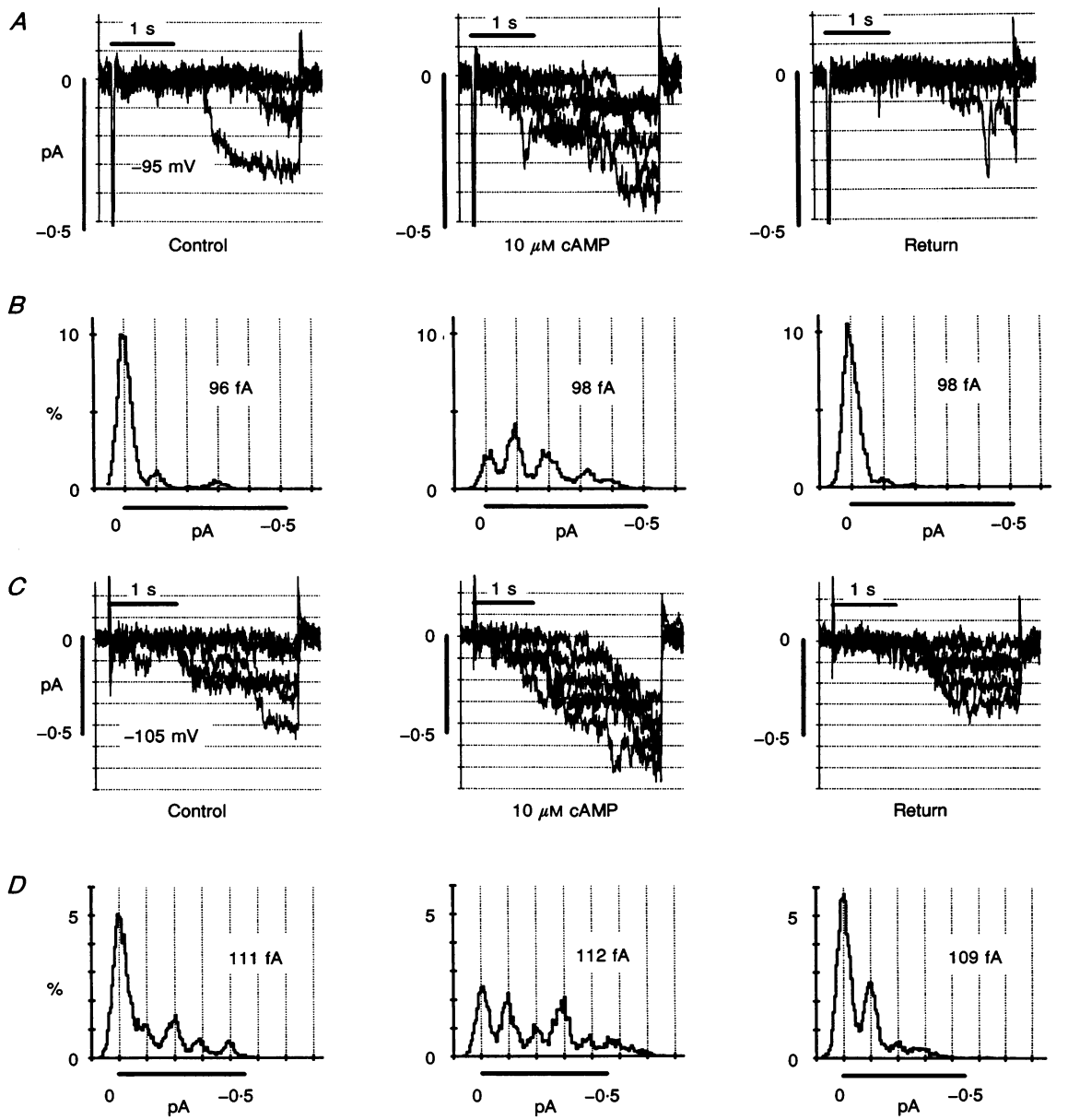

Figure 3. Action of internal cAMP on single i_f channels

A and *C*, current traces recorded during hyperpolarizations of 3 s duration to −95 mV (*A*) and −105 mV (*C*) in an inside-out patch before (left), during (middle) and after (right) perfusion with 10 μM cAMP, as indicated. Six current records are superimposed in each panel. The patch contained at least 11 channels, as derived from the maximal number of openings observed on stepping to −115 mV during cAMP exposure (data not shown). At both voltages, cAMP increased the maximal number of openings observed (from 3 to 4 at −95 mV and from 4 to 6 at −105 mV). *B* and *D*, cumulative histograms of current distributions (bin width = 6 fA) corresponding to records shown on top. Single-channel amplitudes obtained by maximizing histogram areas around peaks (see Methods) were: −96, −98 and −98 fA at −95 mV and −111, −112 and −109 fA at −105 mV before, during and after perfusion with cAMP, respectively.

be satisfactory. Linear regression of inside-out data yielded a single-channel conductance of 0·97 pS and a reversal potential of −2·0 mV (continous line), which compare with the values of 0·98 pS and −13 mV obtained previously from cell-attached measurements (dashed line).

The resolution of elementary events in inside-out patches containing a limited number of channels (< 15) was sufficiently high to allow investigation of the action of cAMP on single i_f channels. To this aim, patches were exposed in sequence to a control solution, a solution containing 10 μM cAMP, and back to the control solution, while single-channel activity was recorded. In Fig. 3 the effect of cAMP is shown on i_f channels during activation at −95 and −105 mV in a patch containing eleven channels.

Comparison of single-channel traces with and without cAMP indicates that cAMP increased the maximal number of channels open (from 3 to 4 at −95 mV; from 4 to 6 at −105 mV) and facilitated channel opening upon hyperpolarization. Selecting records with at least one opening, we measured mean latencies to first opening of 2·15 ± 0·16 s (number of records $n = 8$) and 0·65 ± 0·09 s ($n = 9$) at −95 mV, 1·36 ± 0·17 s ($n = 20$) and 0·66 ± 0·17 s ($n = 7$) at −105 mV, and 0·86 ± 0·11 s ($n = 17$) and 0·40 ± 0·07 s ($n = 6$) at −115 mV (records not shown) in the absence and presence of cAMP, respectively. A more detailed analysis of first latencies is treated below in Fig. 5. Facilitation of channel opening was also apparent from the histogram plots at both voltages (Fig. 3*B* and *D*). In the presence of cAMP, the appearance of records with several openings was favoured, and low-number histogram peak levels were depressed. On the other hand, exposure to cAMP did not alter the single-channel amplitude appreciably at either voltage. Calculation of the single-channel size from each histogram yielded values of −96, −98 and −98 fA at −95 mV, and −111, −112 and −109 fA at −105 mV for control, cAMP and return records, respectively.

The lack of effect of cAMP on the i_f channel conductance was confirmed by comparing single-channel amplitudes in the absence and in the presence of cAMP in several patches, as shown in Fig. 4.

Here, single-channel amplitudes measured from six inside-out patches exposed to a control solution (open squares) and to a solution containing 10 μM cAMP (filled circles) in the range −95 to −115 mV are indeed clustered together around the cell-free single-channel *I–V* relation replotted from Fig. 2. The mean ratio between i_f single-channel amplitudes with and without 10 μM cAMP from the data shown in Fig. 4 was 1·008 ± 0·007 ($n = 9$). The differences between mean control and cAMP single-channel values were not significant ($P > 0·1$) at any of the voltages investigated (−95, −105 and −115 mV).

The data shown above agree with previous evidence that extracellularly perfused adrenaline increases the probability of i_f channel opening but does not vary the single-channel conductance in cell-attached recordings (DiFrancesco, 1986), and that elevation of intracellular cAMP in whole-cell recordings, or direct perfusion of cAMP in inside-out macro-patch recordings, increases the degree of i_f activation without altering its fully activated *I–V* relation (DiFrancesco *et al.* 1986; DiFrancesco & Tromba, 1988*b*; DiFrancesco & Tortora, 1991). Evaluation of the open probability of single i_f channels at steady state would require long, stable recordings in patches containing one channel or at most a few channels (Colquhoun & Hawkes, 1983; Sachs, Neil & Barkakati, 1983). Because of the low i_f single-channel conductance, this could not be achieved satisfactorily. To quantify the changes induced by cAMP on the channel opening process, we used two approaches: (a) the measurement of the distribution of latencies to first opening following hyperpolarization, and (b) the evaluation of steady-state open probability curves in macro-patches containing several channels.

The action of 10 μM cAMP on the cumulative frequency distribution of the latency to first opening (*W*) during hyperpolarization to −105 mV is shown in Fig. 5 for a patch containing no less than sixteen channels. In *A*, four traces are shown before (left) and during (right) perfusion of the internal side of the patch with 10 μM cAMP. The curves have zero current levels shifted with respect to each other for clarity. The shortening of the times to first opening

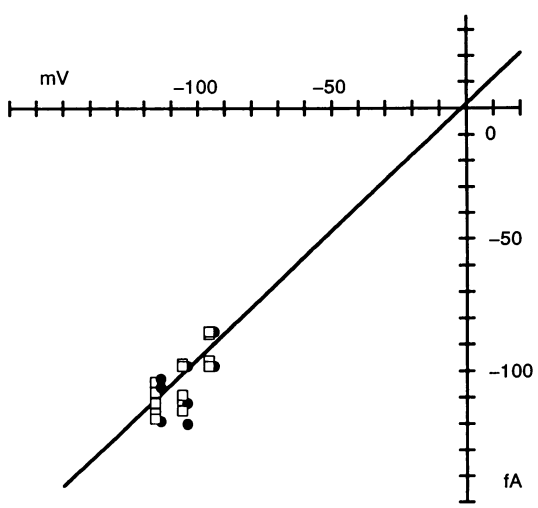

Figure 4. Comparison between amplitudes of elementary single i_f channel currents in the control solution and during perfusion with 10 μM cAMP

Data from 6 patches were collected by fitting histogram peaks as in Fig. 2. The ratio of channel conductance in the presence of cAMP (●) to that in control conditions (□) was 1·008 ± 0·007 ($n = 9$).

(indicated by arrows) during cAMP perfusion is clearly apparent. The cumulative frequency distribution of first openings shown in *B* indicates that cAMP shifted the curve to the left on the time scale, in agreement with the observation that cAMP accelerates channel opening. These curves approximate the probability $W(t)$ that in this patch, channels open by time t since the onset of the hyperpolarizing step to −105 mV. Results similar to those in Fig. 5, indicating a shift to shorter times of the cumulative frequency of first opening latencies, were obtained at −95 mV ($n = 2$), −105 ($n = 3$) and −115 mV ($n = 2$).

For a more direct evaluation of the action of cAMP on the channel open probability at steady state, we used inside-out macro-patches containing hundreds of channels (DiFrancesco & Tortora, 1991) and applied the ramp protocol shown in Fig. 6. The ramp was sufficiently slow to allow the measurement of steady-state current, throughout the voltage range investigated, with adequate accuracy (see

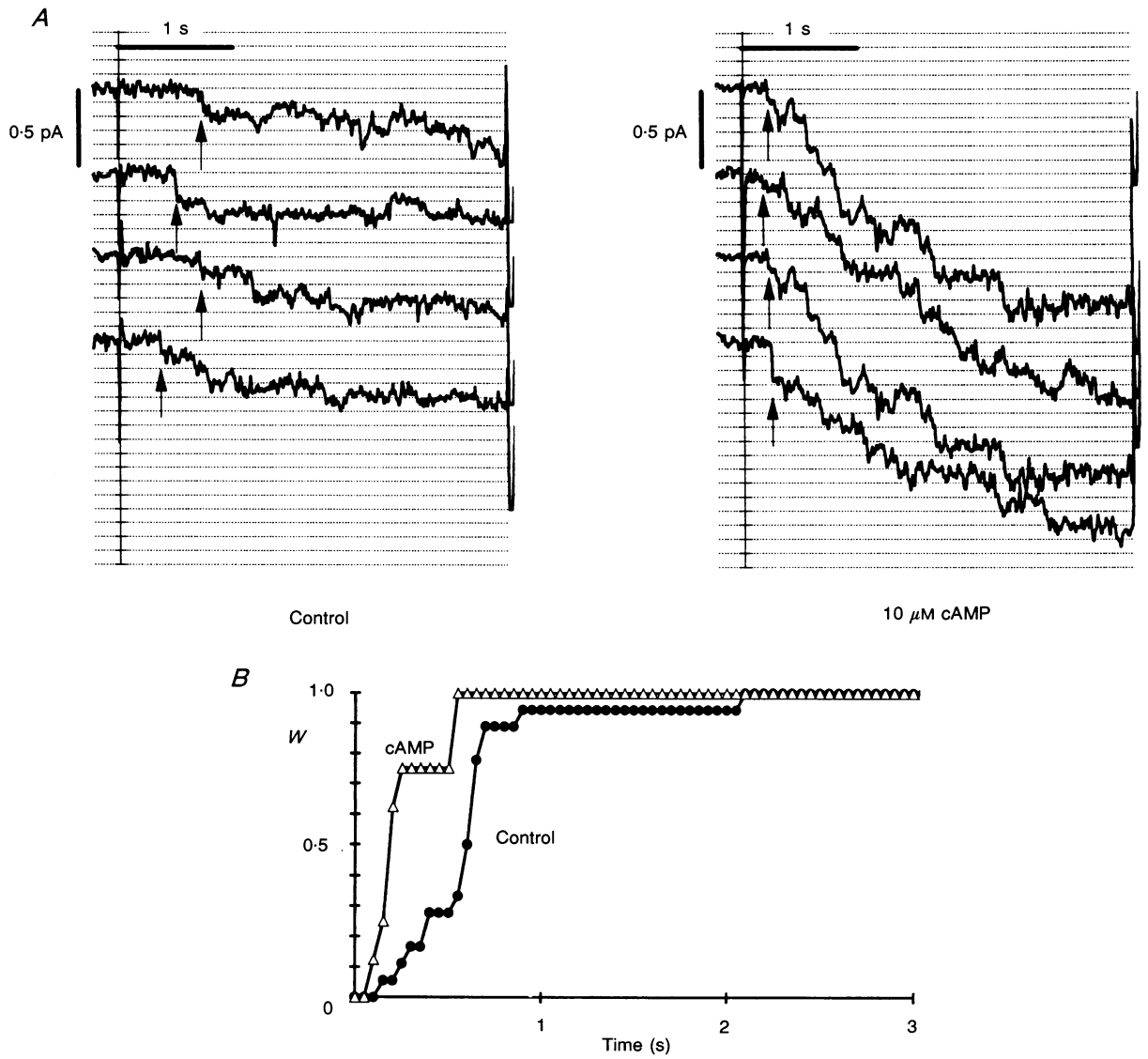

Figure 5. Action of cAMP on latency-to-first-opening histograms
A, current traces recorded upon hyperpolarization to −105 mV from a holding potential of −35 mV from a patch containing no less than 16 channels in a control solution (left) and during perfusion with 10 μM cAMP (right). The single-channel size was −0·097 pA, as determined by amplitude histograms. Traces are shifted vertically (by 6 elementary steps with respect to each other) for clarity. Arrows indicate times where first openings occurred. *B*, cumulative frequency of latency to first opening (W) in a control solution and in the presence of cAMP, as indicated, plotted as a function of time since onset of the hyperpolarization (bin = 50 ms). W was calculated from the non-cumulative distribution of first latencies using eqn (1) (see Methods) from 18 traces in the control solution and 8 traces in the presence of cAMP.

Methods). The currents obtained in control conditions and during cAMP perfusion in Fig. 6 tended to converge at the most negative voltages, as expected if cAMP did not affect the fully activated i_f (DiFrancesco & Tortora, 1991). Activation curves plotted in Fig. 6*C* were calculated as the ratios between measured current and fully activated current, as explained in the Methods (continuous line in *B*: note that time runs backwards in *A* and *B*). Often, but not always, current run-down was observed, which resulted in a depression of maximal current and a shift of the probability curve to the negative direction.

For independently activating channels, the curves plotted in Fig. 6 represent the voltage dependence of the ratio $p_n = p_o/p_m$ between channel open probability (p_o) and its maximal value (p_m) reached at hyperpolarized levels, and are the macro-patch equivalents of the 'activation' curves measured in whole-cell conditions (Noble & Tsien, 1968). Fitting normalized probability curves showed that in

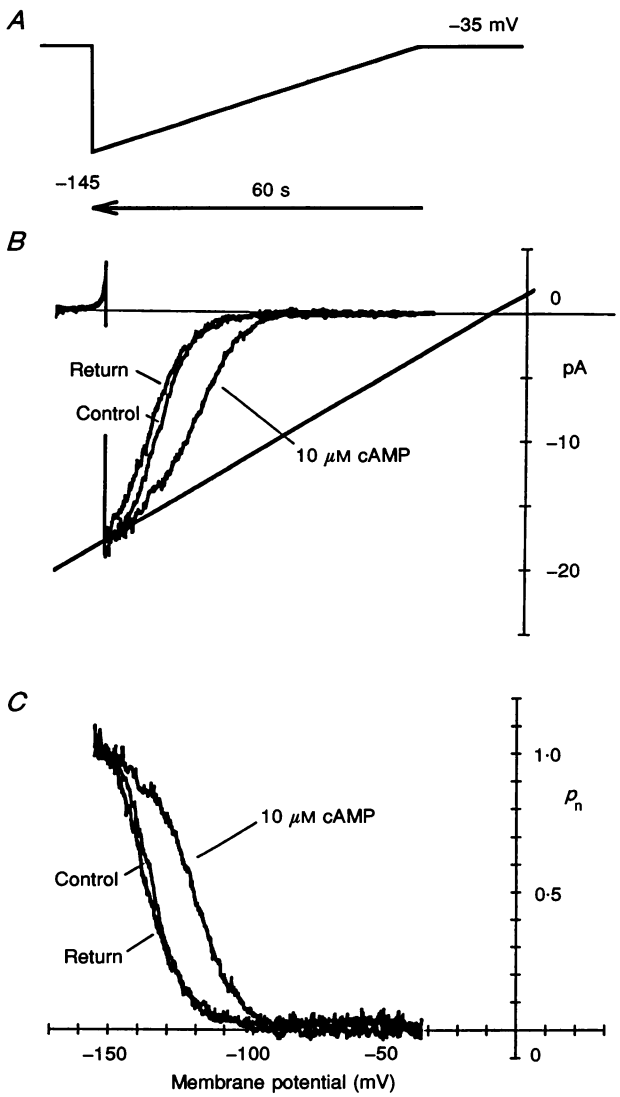

Figure 6. Action of cAMP on the probability of i_f channel opening
A, voltage ramp protocol, consisting of hyperpolarizing ramps from −35 to −145 mV, applied to inside-out patches at a rate of 110 mV min^{-1}. *B*, current elicited by ramp hyperpolarizations before, during and after perfusion with 10 μM cAMP, as indicated. All records were leakage corrected. The patch contained approximately 140 channels. Time runs backwards in *A* and *B* to allow a direct comparison with the curves in *C*. *C*, probability curves calculated as the ratio between the steady-state *I–V* curve and the fully activated relation (straight line in *B*), with the procedure detailed in the Methods. The curves represent the normalized steady-state open probability of single i_f channels on the assumption that channels are independent. Curve fitting by the equation $p_n = 1/(1 + \exp(E - E_{½})/s)$ yielded values of −124·6, −110·4 and −126·3 mV for the mid-activation voltage ($E_{½}$) and 6·42, 7·36 and 6·13 mV for the inverse-slope factor (s) before, during and after 10 μM cAMP, respectively.

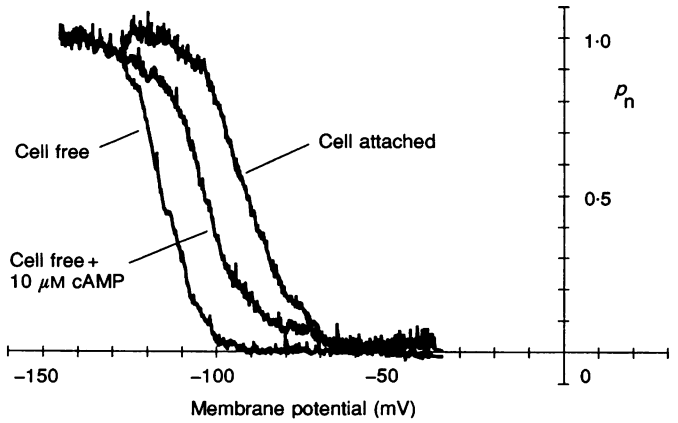

Figure 7. Comparison of open probability curves in cell-free and cell-attached conditions
Curves were constructed using 110 mV min^{-1} hyperpolarizing ramp protocols applied to an inside-out, cell-free macro-patch in the standard control solution and during perfusion with 10 μM cAMP, and to a different macro-patch in the cell-attached configuration, as indicated. The cell-attached curve was measured during cell superfusion with a high K^+ solution (see Methods) to reduce the resting membrane potential to zero, by applying inverted resting and ramp potentials to the patch pipette. Best fitting with the same equation as in Fig. 6 yielded the values $E_{½} = -115·3$, $-103·2$ and $-85·5$ mV and $s = 5·40$, 6·34 and 9·39 mV for the cell-free control and cAMP curve, and for the cell-attached curve, respectively.

the experiment of Fig. 6, 10 μM cAMP reversibly shifts the mid-point of the i_f probability curve ($E_{½}$) by 14·2 mV from −124·6 to −110·4 mV, and moderately increases the inverse slope coefficient (s) from 6·42 to 7·36 mV. In fourteen patches, $E_{½}$ was $-121·9 \pm 1·6$, $-108·7 \pm 1·7$ and $-122·3 \pm 1·7$ mV, and s was $6·18 \pm 0·23$, $6·40 \pm 0·28$ and $5·94 \pm 0·33$ mV before, during and after 10 μM cAMP, respectively.

Thus, cAMP shifted the probability curve by an average 13·2 mV (statistically significant: $P < 0·01$) and did not affect its steepness significantly ($P > 0·05$). The measured shift was slightly larger than that of 10·4 mV obtained previously with 10 μM cAMP (DiFrancesco & Tortora, 1991); this difference may be due to the different protocols used in the two measurements. The shift of 13·2 mV is also comparatively larger than that of 7·8 mV obtained with 1 μM isoprenaline in whole-cell experiments (DiFrancesco & Tortora, 1991). A possible reason for this difference is mentioned in the Discussion.

The position of the i_f open probability curve was substantially more negative than that of the activation curve measured in whole-cell experiments (DiFrancesco *et al.* 1986; Denyer & Brown, 1990). On the other hand, significantly more depolarized positions were obtained for probability curves measured in cell-attached conditions with ramp protocols as in Fig. 6. In Fig. 7, the probability curves measured in a cell-free, macro-patch ramp experiment before and during cAMP perfusion are compared with the probability curve measured in cell-attached conditions in a different macro-patch. The half-activation points were −115·3, −103·2 and −85·5 mV for the cell-free control and cAMP curves and for the cell-attached curve, respectively. This comparison suggests that cAMP is unable to recover the entire negative shift which the curve undergoes when patches are extruded from membranes. This observation was confirmed by a more extended comparison. In seven cell-attached patches, ramp protocols as in Fig. 6 yielded curves with mean mid-activation voltage $E_{½} = -91·2 \pm 4·2$ mV and inverse-slope factor $s = 8·0 \pm 0·5$ mV. The 30·7 mV difference between $E_{½}$ values in cell-attached and cell-free measurements could be only partly attributed to a basal level of intracellular cAMP in cell-attached conditions, as shown by the fact that saturating concentrations of cAMP (100 μM) displaced $E_{½}$ by $14·6 \pm 0·6$ mV ($n = 2$), a shift only slightly larger than that of 13·2 mV obtained with 10 μM cAMP. The difference between cell-free and cell-attached i_f activation ranges, together with the observation that the position of the open probability curve slowly drifted to the left during measurements, suggest that a run-down process independent of cAMP may contribute to the hyperpolarized position of the probability curve in cell-free patches.

DISCUSSION

Our data represent a direct indication that cAMP activates i_f channels by facilitating channel opening without altering the single-channel conductance. This is in agreement with previous findings: in whole-cell conditions, β-adrenergic/muscarinic stimulation or other interventions increasing/decreasing intracellular cAMP act by shifting the i_f activation curve to more positive/negative voltages without modifying the fully activated current (DiFrancesco *et al.* 1986; DiFrancesco & Tromba, 1989); similarly, direct perfusion with cAMP of the intracellular side of inside-out macro-patches increases the degree of i_f activation but leaves unaltered its fully activated I–V relation (DiFrancesco & Tortora, 1991); finally, in cell-attached single i_f channel measurements, externally perfused adrenaline increases opening probability and does not modify the single-channel conductance (DiFrancesco, 1986). Our data indicate that the direct, phosphorylation-independent action of cAMP on single i_f channels is analogous to that observed in cell-attached conditions during cell superfusion with adrenaline. Furthermore, the shifts observed during cAMP perfusion of the intracellular side of macro-patch membranes are comparable with those observed in whole-cell conditions during exposure to catecholamines and acetylcholine (see below). These data favour the view that the major action of β-adrenergic stimulation and of muscarinic inhibition on SA node i_f occurs via adenylate cyclase and cAMP, although they do not exclude the possible presence of other pathways such as a direct, G-protein-mediated mechanism (Yatani & Brown, 1990).

cAMP-induced activation of i_f channels occurs by a shift of the normalized open probability curve to more positive voltages, in agreement with the original finding of the cAMP action on the pacemaker current activation curve (Tsien, 1977). In contrast with previous evidence (Tsien, 1974), however, our data indicate that cAMP does not increase the curve steepness. This difference may be related to the presence of effects of adrenaline other than those directly mediated by cAMP.

The shift of 14·6 mV caused by 100 μM cAMP on the open probability curve is higher than that of 7·8 mV caused by β-adrenergic stimulation on the activation curve in whole-cell conditions with high (1 μM) doses of isoprenaline (DiFrancesco & Tortora, 1991). A lower isoprenaline-induced shift in whole-cell conditions is to be expected as a consequence of the basal cytoplasmic cAMP concentration existing in SA node myocytes. The presence of a substantial basal activity of adenylate cyclase in these cells is suggested by the direct inhibitory effect of muscarinic stimulation on i_f, which is known to be mediated by a decrease of intracellular cAMP (DiFrancesco & Tromba, 1988*b*). Thus, summing up the maximal negative shift induced by ACh (7·2 mV, DiFrancesco, Ducouret & Robinson, 1989) and the maximal positive shift of 7·8 mV induced by catecholamines gives the figure of 15·0 mV which is more directly comparable with the maximal shift of 14·6 mV produced by cAMP.

The agreement between maximal shift values obtained by direct cAMP application on the intracellular side of the membrane and by extracellular receptor stimulation supports the view that in the SA node myocyte, basal adenylate cyclase activity keeps the cAMP level approximately in the middle of the range of cAMP concentrations interacting with the i_f channel (about 0·2 μM according to the macro-patch dose–response relationship, DiFrancesco & Tortora, 1991). At this level the i_f sensitivity to cAMP is maximal, so that small variations of cAMP concentration will be able to modify the degree of current activation substantially and consequently affect the spontaneous rate of pacemaker activity.

The maximal effect of saturating cAMP doses is too reduced, on the other hand, to account for all of the difference between half-activation voltages in cell-attached and cell-free conditions (30·2 mV). This implies that mechanisms other than the direct cAMP-activating action may operate to keep the normal voltage dependence of the i_f activation curve. The evidence that, as in the run-down phenomenon in whole-cell conditions, the position of the i_f open probability curve shifts progressively to the left after patch excision in cell-free patches suggests that processes operating in the intact cell to maintain i_f channels in the normal working state are disrupted after patch excision. This may explain why, for example, inhibition of phosphorylating processes by unspecific protein kinase inhibitors affects the normal response of the i_f current to neurotransmitters in Purkinje fibres (Chang, Cohen, DiFrancesco, Rosen & Tromba, 1991).

Voltage shifts of kinetic parameters to the negative direction, due to run-down, have been reported for Na^+ and Ca^{2+} channels (Belles, Malécot, Hescheler & Trautwein, 1988; Hanck & Sheets, 1992; Ono, Fozzard & Hanck, 1993). For Na^+ channels, the mechanism underlying the run-down shift appears to be different from that originated by cAMP-mediated channel phosphorylation (Ono *et al.* 1993), whereas for Ca^{2+} channels phosphorylation inhibits current run-down (Ono & Fozzard, 1992). The negative shift of the i_f activation curve in cell-free conditions is unlikely to be due to a phosphorylation process, because the solutions we used to perfuse the intracellular side of the membrane patch did not contain Mg-ATP.

As a simple shift of the voltage dependence of the open probability curve, the action of cAMP is indistinguishable from that originated by an increase in the voltage drop sensed by the gating mechanism. It is an attractive speculation that cAMP and voltage act on the i_f channel gate sensor similarly, possibly by stabilizing a conformational change that favours channel opening.

REFERENCES

Belles, B., Malécot, C. O., Hescheler, J. & Trautwein, W. (1988). 'Run-down' of the Ca current during long whole-cell recordings in guinea-pig heart cells: role of phosphorylation and intracellular calcium. *Pflügers Archiv* **411**, 353–360.

Brown, H. F., DiFrancesco, D. & Noble, S. J. (1979). How does adrenaline accelerate the heart? *Nature* **280**, 235–236.

Chang, F., Cohen, I. S., DiFrancesco, D., Rosen, M. R. & Tromba, C. (1991). Effects of protein kinase inhibitors on canine Purkinje fibre pacemaker depolarization and the pacemaker current i_f. *Journal of Physiology* **440**, 367–384.

Colquhoun, D. & Hawkes, A. G. (1983). The principles of the stochastic interpretation of ion-channel mechanisms. In *Single Channel Recording*, ed. Sackmann, B. & Neher, E., pp. 135–175. Plenum Press, New York.

Denyer, J. C. & Brown, H. F. (1990). Rabbit isolated sino-atrial node cells: isolation and electrophysiological properties. *Journal of Physiology* **429**, 405–424.

De Peyer, J. E., Cachelin, A. B., Levitan, I. B. & Reuter, H. (1982). Ca^{2+}-activated K^+ conductance in internally perfused snail neurons is enhanced by protein phosphorylation. *Proceedings of the National Academy of Sciences of the USA* **79**, 4207–4211.

DiFrancesco, D. (1986). Characterization of single pacemaker channels in cardiac sino-atrial node cells. *Nature* **324**, 470–473.

DiFrancesco, D. (1991). The contribution of the hyperpolarization-activated current (i_f) to the generation of spontaneous activity in rabbit sino-atrial node myocytes. *Journal of Physiology* **434**, 23–40.

DiFrancesco, D. (1993). Pacemaker mechanisms in cardiac tissue. *Annual Review of Physiology* **55**, 451–467.

DiFrancesco, D., Ducouret, P. & Robinson, R. B. (1989). Muscarinic modulation of cardiac rate at low acetylcholine concentrations. *Science* **243**, 669–671.

DiFrancesco, D., Ferroni, A., Mazzanti, M. & Tromba, C. (1986). Properties of the hyperpolarizing-activated current (i_f) in cells isolated from the rabbit sino-atrial node. *Journal of Physiology* **377**, 61–88.

DiFrancesco, D. & Noble, D. (1988). Current i_f and its contribution to cardiac pacemaking. In *Cellular and Neuronal Oscillators*, ed. Jacklet, J. W., pp. 31–57. Marcel Dekker, New York.

DiFrancesco, D. & Tortora, P. (1991). Direct activation of cardiac pacemaker channels by intracellular cyclic AMP. *Nature* **351**, 145–147.

DiFrancesco, D. & Tromba, C. (1988*a*). Inhibition of the hyperpolarization-activated current, i_f, induced by acetylcholine in rabbit sino-atrial node myocytes. *Journal of Physiology* **405**, 477–491.

DiFrancesco, D. & Tromba, C. (1988*b*). Muscarinic control of the hyperpolarization-activated current i_f in rabbit sino-atrial node myocytes. *Journal of Physiology* **405**, 493–510.

DiFrancesco, D. & Tromba, C. (1989). Channel activity related to pacemaking. In *Isolated Adult Cardiomyocytes*, vol. II, ed. Isemberg, G. & Piper, H. M., pp. 97–115. CRC Press Ltd, Boca Raton, FL, USA.

Hanck, D. A. & Sheets, M. F. (1992). Time-dependent changes in kinetics of Na^+ current in single canine cardiac Purkinje cells. *American Journal of Physiology* **262**, H1197–1207.

Levitan, I. B. (1985). Phosphorylation of ion channels. *Journal of Membrane Biology* **87**, 177–190.

Noble, D. & Tsien, R. W. (1968). The kinetics and rectifier properties of the slow potassium current in calf Purkinje fibres. *Journal of Physiology* **195**, 185–214.

Noma, A., Kotake, H. & Irisawa, H. (1980). Slow inward current and its role mediating the chronotropic effect of epinephrine in the rabbit sinoatrial node. *Pflügers Archiv* **388**, 1–9.

Ono, K. & Fozzard, H. A. (1992). Phosphorylation restores activity of L-type calcium channels after run-down in inside-out patches from rabbit cardiac cells. *Journal of Physiology* **454**, 673–688.

Ono, K., Fozzard, H. A. & Hanck, D. A. (1993). Mechanism of cAMP-dependent modulation of cardiac sodium channel current kinetics. *Circulation Research* **72**, 807–815.

Osterrieder, W., Brum, G., Hescheler, J., Trautwein, W., Flockerzi, V. & Hoffmann, F. (1982). Injection of subunits of cyclic AMP dependent protein kinase into cardiac myocytes modulates Ca^{2+} current. *Nature* **298**, 576–578.

Reuter, H. (1983). Calcium channel modulation by neurotransmitters, enzymes and drugs. *Nature* **301**, 569–574.

Sachs, F., Neil, J. & Barkakati, N. (1983). The automated analysis of data from single ionic channels. *Pflügers Archiv* **395**, 331–340.

Shuster, M. J., Camardo, J. S., Siegelbaum, S. A. & Kandel, E. R. (1985). Cyclic AMP-dependent protein kinase closes the serotonin-sensitive K^+ channels of *Aplysia* sensory neurones in cell-free membrane patches. *Nature* **313**, 392–395.

Tsien, R. W. (1974). Effect of epinephrine on the pacemaker potassium current of cardiac Purkinje fibers. *Journal of General Physiology* **64**, 293–319.

Tsien, R. W. (1977). Cyclic AMP and contractile activity in heart. *Advances in Cyclic Nucleotide Research* **8**, 363–420.

Yatani, A. & Brown, A. M. (1990). Regulation of cardiac pacemaker current i_f in excised membranes from sinoatrial node cells. *American Journal of Physiology* **258**, H1947–1951.

Yatani, A., Okabe, K., Codina, J., Birnbaumer, A. & Brown, A. M. (1990). Heart rate regulation by G-protein acting on the cardiac pacemaker channel. *Science* **249**, 1163–1166.

Acknowledgements

We thank Mirko Baruscotti for assistance, Antonio Zaza, Gianmaria Maccaferri and Arnaldo Ferroni for discussion and Mr G. Mostacciuolo for technical help. This work was supported by the Consiglio Nazionale delle Ricerche (grant CT04 91.00722 to D.D.).

Received 24 March 1993; accepted 14 July 1993.